

Standard Definitions of Persistence Length Do Not Describe the Local “Intrinsic” Stiffness of Real Polymer Chains

Hsiao-Ping Hsu,^{*,†} Wolfgang Paul,^{†,‡} and Kurt Binder[†]

[†]*Institut für Physik, Johannes Gutenberg-Universität Mainz, Staudinger Weg 7, D-55099 Mainz, Germany, and*

[‡]*Theoretische Physik, Martin Luther Universität Halle-Wittenberg, von Senckendorffplatz 1, 06120 Halle, Germany*

Received December 9, 2009; Revised Manuscript Received February 5, 2010

ABSTRACT: On the basis of extensive Monte Carlo simulations of lattice models for linear chains under good and Θ solvents conditions, and for bottle-brush polymers under good solvent conditions, different methods to estimate the persistence lengths of these polymers are applied and compared to each other. While for chain molecules at the Θ point standard textbook definitions of the persistence length yield consistent results, under good solvent conditions the persistence length (according to its standard definitions) diverges when the chain length of the macromolecules tends to infinity. Accurate simulation results for chain lengths up to $N_b = 6400$ allow us to verify the theoretically predicted power laws for the decay of the bond orientational correlation function. For the case of bottle-brush polymers, this dependence of “the” persistence length on the backbone chain length obscures the dependence on the side chain length, that is controversially discussed in the literature. Alternative definitions of a persistence length that do not suffer from this problem, based on the total linear dimension of the chain or on the scattering function via the so-called “Holtzer plateau” are studied as well. We show that the backbone contour length of the bottle-brush needs to be very large (about 100 persistence lengths in typical cases) to reach the asymptotic limit where the bottle-brush satisfies the self-avoiding walk statistics, and where a well-defined persistence length can be extracted. An outlook to pertinent experimental work is given.

1. Introduction

One of the most basic characteristics of macromolecules is the flexibility of the polymer chains. As is emphasized in standard textbooks (e.g., on p 3 of ref 1), “any long macromolecule is flexible, but different polymers have different mechanisms of flexibility”, and discussing various models obeying Gaussian statistics one finds that (p 5 of ref 1) “the directional correlation of two segments of a macromolecule diminishes exponentially with the growth of the chain length separating them”. Thus, the mean cosine between two segments separated by a distance s/l_b along the chain can be written as (where $s = |i - j|$ and $l_b = |\vec{a}_i|$ with $\vec{a}_i = \vec{r}_i - \vec{r}_{i-1}$ where \vec{r}_i is the position of the i th monomer in space)

$$\langle \cos \Theta(s) \rangle = \langle \vec{a}_i \cdot \vec{a}_j \rangle / l_b^2 = \exp(-s/l_p) \quad (1)$$

where^{1–3} the persistence length l_p is taken as the basic characteristics of polymer flexibility. For flexible chains, one expects that l_p is of the same order as l_b , while for semiflexible chains (e.g., described by the Kratky–Porod⁴ “worm-like chain” model) $l_p \gg l_b$. For ideal chains $\langle \cos \Theta(s) \rangle = \langle \cos \Theta \rangle^s$ (where $\langle \cos \Theta(1) \rangle$ is abbreviated as $\langle \cos \Theta \rangle$) and for large l_p one has $\langle \cos \Theta \rangle \approx 1 - 1/2\langle \Theta^2 \rangle$ and $l_p = 2/l_b\langle \Theta^2 \rangle$. The mean square end-to-end distance of such semiflexible ideal chains can be written as (the number of bonds $N_b \gg 1$ henceforth is denoted as “chain length”)

$$\langle R_e^2 \rangle = N_b l_b^2 \frac{1 + \langle \cos \Theta \rangle}{1 - \langle \cos \Theta \rangle} = C_{\infty} l_b^2 N_b \approx \frac{4}{\langle \Theta^2 \rangle} l_b^2 N_b \quad (2)$$

*Corresponding author.

Defining a Kuhn step length^{1–3} l_k via the equivalent freely jointed chain ($\langle R_e^2 \rangle = n l_k^2$, $n l_k = N_b l_b$) one readily concludes that the persistence length is equal to one-half the Kuhn length,

$$l_p = \frac{1}{2} l_k = 2/l_b \langle \Theta^2 \rangle \quad (3)$$

Equations 1–3 are used routinely in experimental work, although they hold only for “ideal chains” obeying Gaussian statistics, and not necessarily for real polymer chains. But it is known that for dilute solutions at the Θ point, where the excluded volume repulsion is effectively canceled by solvent-mediated attractive forces between the monomers, one still has

$$\langle R_e^2 \rangle \propto l_b^2 N_b \quad (4)$$

when logarithmic corrections^{5,6} are disregarded. Hence, it was believed that eqs 1, 3 still hold for chains at the Θ point. A similar cancellation is believed to hold for chains in dense melts (“Flory hypothesis”)^{7,8} as well.

However, the applicability of eqs 1 and 3 for chains in dense melts and in Θ solutions has recently been called into question by the finding that bond-orientational correlations show a power law decay rather than an exponential decay, both for dense melts^{9,10} and at the Θ point,¹¹

$$\langle \cos \Theta(s) \rangle \propto s^{-3/2}, \quad s^* < s \ll N_b \quad (5)$$

Shirvanyants et al.¹¹ suggest that for $s < s^*$ eq 1 still can be used and estimate that the crossover index $s^* \propto l_p/l_b$; but clearly it becomes difficult to disentangle where eq 1 would still be applicable if l_p is not much larger than l_b .

Now, an alternative definition of the persistence length due to Flory^{12,13} does not postulate a specific form for $\langle \cos \Theta(s) \rangle$ and

actually allows to define a persistence length locally for any bond along a chain,

$$l_p(k)/l_b = \langle \vec{a}_k \cdot \vec{R}_e / |\vec{a}_k|^2 \rangle, \quad k = 1, \dots, N_b \quad (6)$$

One expects that $l_p(k)$ is reduced near the chain ends, but should reach actually a flat plateau, essentially independent of k , in the chain interior. If this happens, this plateau value resulting from eq 6 actually is a useful measure for the intrinsic chain stiffness.

However, often polymers are studied under good solvent conditions^{1-3,6-8} and then both eqs 1 and 6 are unsuitable to characterize the local “intrinsic” stiffness of a chain. Using renormalization group methods,^{3,6,8} Schäfer et al.¹⁴ have shown that to a very good approximation

$$l_p(k)/l_b \approx \alpha [k(N_b - k)/N_b]^{2\nu - 1} \quad (7)$$

where α is a (nonuniversal) constant and ν is the exponent characterizing chain linear dimensions in good solvents,^{1-3,6-8}

$$\langle R_e^2 \rangle \propto N_b^{2\nu}, \quad \nu \approx 0.588. \quad (8)$$

From eq 7 we immediately recognize that $l_p(k)$ is not flat in the chain interior, but rather shows a convex variation around the maximum at $k = N_b/2$, with

$$l_{p,\max}(k) \approx l_b \alpha (N_b/4)^{2\nu - 1} \rightarrow \infty \text{ as } N_b \rightarrow \infty \quad (9)$$

Similarly, in the good solvent regime, neither eq 1 nor eq 5 hold, but rather¹⁴

$$\langle \cos \Theta(s) \rangle \propto s^{-\beta}, \quad s^* < s \ll N_b, \quad \beta = 2 - 2\nu \approx 0.824 \quad (10)$$

If, in view of the difficulty of understanding the decay law of $\langle \cos \Theta(s) \rangle$ in the different regimes, one chooses an alternative “integral definition”¹⁵

$$l'_p = l_b \sum_{s=1}^{N_b} \langle \cos \Theta(s) \rangle \approx l_b \int_0^{N_b} ds \langle \cos \Theta(s) \rangle \quad (11)$$

one recovers $l'_p = l_p$ if eq 1 holds (and for $N_b \gg l_p$). A finite value of l'_p (independent of N_b for large N_b) also results for Θ chains and dense melts (where eq 5 holds), while in the good solvent case eqs 10, 11 lead to

$$l'_p \propto N_b^{2\nu - 1} \quad (12)$$

consistent with eq 9. Interestingly, if one still applied the definition of the Kuhn step length also in the good solvent regime, one would obtain a related scaling

$$l_k = s \langle R_e^2 \rangle / (N_b l_b) \propto N_b^{2\nu - 1} \quad (13)$$

implying that we still would have $l_{p,\max}(k) \propto l'_p \propto l_k$, although neither of these lengths is useful as a measure of the local intrinsic stiffness of the chain. In view of this situation, Hsu et al.^{15,17} proposed to simply define a persistence length (l''_p) via the mean square end-to-end distance (or, alternatively, the mean square radius of gyration $\langle R_g^2 \rangle$)¹⁷

$$\langle R_e^2 \rangle = 2l''_p l_b N_b^{2\nu}, \quad N_b \rightarrow \infty \quad (14)$$

Note that for ideal chains (no excluded volume) $\nu_{id} = 1/2$ and therefore we have for semiflexible ideal chains from

eqs 2 and 3

$$\langle R_e^2 \rangle = 2l_b l_p N_b^{2\nu_{id}}, \quad \langle R_g^2 \rangle = \frac{1}{6} \langle R_e^2 \rangle = \frac{1}{3} l_p l_b N_b^{2\nu_{id}} \quad (15)$$

Thus, l''_p also reduces to the standard persistence length l_p if the chains are ideal, but remains a finite length (asymptotically independent of N_b for $N_b \rightarrow \infty$) if we take eq 14 as a natural generalization of eq 15 to the excluded volume case where $\nu > \nu_{id}$.

For all the definitions of persistence lengths discussed so far, it is rather important that the limit of very long chains, $N_b \rightarrow \infty$, is considered. This is inconvenient, since (particularly in the good solvent case) the approach to this limit can be rather slow; so in practice “corrections to scaling”^{3,6} may need consideration when one applies eq 14. In addition, often one is interested in rather short relatively stiff chains, where the contour length $L = N_b l_b$ exceeds l''_p only by a factor of order unity, rendering eq 14 inapplicable. For ideal Kratky–Porod chains the corresponding generalization of eq 15 is^{3,4}

$$\langle R_e^2 \rangle = 2l_b l_p N_b \left\{ 1 - \frac{l_p}{N_b l_b} [1 - \exp(-N_b l_b / l_p)] \right\} \quad (16)$$

leading to $\langle R_e^2 \rangle \approx (N_b l_b)^2 = L^2$ in the limit $l_p \gg N_b l_b$, as expected for straight rods of length L . While this latter result also holds in the excluded volume case, the crossover from eq 14 to $\langle R_e^2 \rangle = N_b^2 l_b^2$ with increasing l''_p is not described by a simple formula such as eq 16.

But an alternative approach to obtain persistence lengths, useful also when chains are not very long, rests on the study of the structure factor $S(q)$, which is defined by (note that we have N_b bonds and hence $N_b + 1$ monomers in a chain)¹⁻³

$$S(q) = \frac{1}{(N_b + 1)^2} \left\langle \sum_{j=0}^{N_b} \sum_{k=0}^{N_b} \exp[i\vec{q} \cdot (\vec{r}_j - \vec{r}_k)] \right\rangle \quad (17)$$

For small q , eq 17 always can be written as

$$S(q \rightarrow 0) = 1 - \frac{1}{3} q^2 \langle R_g^2 \rangle + \dots \quad (18)$$

For an ideal Porod–Kratky^{3,4} chain, $S(q)$ can be calculated^{3,18} for all q , but a simple result is only obtained in the limit $N_b l_b / l_p \gg 1$ and large q ,¹⁸ namely $q l_p \geq 3$,

$$N_b q l_b S(q) = \pi + \frac{2}{3} \frac{1}{(q l_p)} \quad (19)$$

Equation 19 has been used by Lecommandoux et al.¹⁹ to extract persistence lengths of polymers with bottle-brush architecture.^{20,21} This equation has a simple interpretation in terms of the scattering from rigid rods of length L , which is described by²²

$$S_{\text{rod}}(q, L) = \frac{2}{qL} \int_0^{qL} \left(\frac{\sin t}{t} \right) dt - 4 \frac{\sin^2 \left(\frac{1}{2} qL \right)}{(qL)^2} \quad (20)$$

For $qL \rightarrow \infty$, eq 20 reduces simply to $\pi/(qL)$, i.e. the first term on the right-hand side of eq 19. This observation already suggests that if a polymer over some length scales from l_b to l_p with $l_p \gg l_b$ behaves as a locally stiff object, one should expect to see in the scattering function when multiplied with q a flat region from about $q \approx l_p^{-1}$ to about $q \approx l_b^{-1}$. This so-called “Holtzer plateau”^{23,24} hence can serve to extract the contour length $L = N_b l_b$ of the chain from the scattering, and the above argument suggests

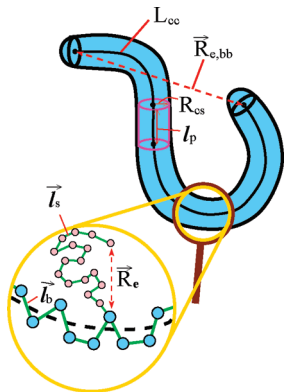


Figure 1. Multitude of length scales for molecular bottle-brush polymers. A coarse-grained description depicts the object as a flexible spherocylinder (upper part) with a cross-sectional radius R_{cs} and contour length L_{cc} along the axis of the coarse-grained cylinder. The end-to-end distance of the backbone is $R_{e,bb}$. Over a length scale l_p the cylinder is stiff while on larger length scales it bends. On a less coarse-grained view (lower part) the backbone forms a self-avoiding walk formed by N_b bond vectors l_b . Side chains of length N_s (with bond vectors l_s) and end-to-end distance R_e are grafted (grafting density σ) at the (effective) monomers of the backbone.

that this method should be valid also in the presence of excluded volume interactions. The onset of this “Holtzer plateau” in q -space then gives some (at least semiquantitative) information on l_p .

Finally, we mention an interesting attempt to construct $S(q)$ for semiflexible polymers numerically due to Pedersen and Schurtenberger.²⁵ Using a discrete representation of the wormlike chain model, putting N_b spheres of radius $R = 0.1b$ at distance l_b at a contour with $L = N_b l_b$ and $b = l_b(1 + \cos \Theta)/(1 - \cos \Theta)$, where Θ is the valence angle; thus, b plays the role of the statistical segment length. Careful Monte Carlo simulations were performed for a wide range of values for L/b , and the simulated structure factors $S(q)$ have been fitted to an empirical function of the type

$$S(q, L, b) = \{[1 - \chi(q, L, b)]S_{\text{chain}}(q, L, b) + \chi(q, L, b)S_{\text{rod}}(q, L)\}\Gamma(q, L, b) \quad (21)$$

where $S_{\text{chain}}(q, L, b)$ describes the scattering from a flexible chain (with excluded volume statistics), and $\chi(q, L, b)$ is another function to describe the crossover between $S_{\text{chain}}(q, L, b)$ and the rod-like scattering [eq 20]. The function $\Gamma(q, L, b)$ was found to be necessary to correct the behavior of $S(q, L, b)$ in the crossover region. We do not give the details of this approach here, since it is rather complicated (the quoted functions were parametrized with up to 35 constants²⁵), but emphasize that this function did provide also very good fits to experimental data, such as scattering data from atactic polystyrene dissolved in the good solvent carbon disulfide, and the resulting fit parameters (e.g., $b = 2.48$ nm) seem to be consistent with other information.

This last approach²⁵ to estimate a statistical segment length b has become the method of choice for the analyses of scattering data for bottle-brush polymers.^{24,26,27} This problem is of particular interest, since the structure is characterized by a multitude of length scales (Figure 1), and varying the lengths of the side chains the stiffness of the bottle-brush can be varied over a wide range. However, the theoretical predictions about this variation^{28–39} are controversial, as well as the validity of the persistence length estimates extracted from experiment.^{16,21,24,26,27} The experiments identify the length b resulting from the fit with the Kuhn step length l_k and apply $l_p = l_k/2$ [eq 3] to identify a persistence length, although this relation is only well-established

for ideal chains following Gaussian chain statistics. The problem that in the good solvent case several classical definitions of persistence lengths {via the decay of $\langle \cos \Theta(s) \rangle$, eq 1, or via eq 6, respectively} diverge with N_b as $N_b \rightarrow \infty$ and hence are unsuitable for estimating the range of local intrinsic stiffness is not considered by the theories that consider how l_p scales with the length of side chains.^{28,30–32} It is also not considered by the many studies where persistence lengths for semiflexible chains were estimated from simulations or experiments, e.g. refs 33–43.

In view of this unsatisfactory situation, we present in this paper a comparative study of several definitions of a persistence length for bottle-brush polymers, for which the local intrinsic stiffness can be widely varied via changing the length N of the side chains. Since for short side chain length (such as $N = 6$) a crossover to the behavior of ordinary flexible polymer chains sets in, we present for comparison also a careful study of the ordinary self-avoiding walk model (SAW)^{8,43} on the simple cubic lattice under good solvent conditions (section 2). We also study the same model at the Θ temperature (section 2). While both models have been studied before,^{11,14} our work extends these studies considerably since we study much longer chains and obtain also much better statistical accuracy than was reached in previous simulations. This is possible since our model can be studied very efficiently with the pruned–enriched Rosenbluth method (PERM).⁴⁵ Related work on bond orientational correlations in melts^{9,10} shows that chain lengths $N_b \geq 10^3$ are crucial for a convincing test of the theory. In section 3, we give a study of the bond fluctuation model^{46–48} of bottle-brush polymers with flexible backbone, extending previous work.^{15,16}

The aim of our paper hence is to provide guidance to future work (both experiment, simulation and analytical theory) that addresses the issue of the length scale over which a semi flexible macromolecule (or macromolecular aggregate such as cylindrical micelles, for instance) can be treated like a stiff object. Section 4 then summarizes our conclusions and addresses questions that remain still open.

2. Persistence Lengths for the Standard Self-Avoiding Walk (SAW) and for the Corresponding Model at the Θ Point

Simulations have been carried out for standard SAW’s on the simple cubic lattice for chain lengths N_b up to $N_b = 6400$. Both the case where only excluded volume interaction is present (very good solvent conditions) and the case of chains under Θ conditions (which occur when a nearest-neighbor attraction ϵ is present, such that the parameter $q \equiv \exp(\epsilon/k_B T)$ takes the value $q_\Theta = 1.3087^{45}$) are studied with the PERM algorithm.⁴⁵ We use the lattice spacing as the unit of length, and hence $l_b = 1$ for this model.

Figure 2 shows our results for $\langle \cos \Theta(s) \rangle$ vs s in log–log form, and the fits to the theoretical power laws {eq 10 in the good solvent case and eq 5 in the Θ solvent case, respectively} are shown as straight lines. As expected, there are systematic deviations for small s , the power law should hold only for $s \gg 1$. On the other hand, the power law is only seen for s about an order of magnitude smaller than N_b : Thus, one sees that for $N_b = 400$ significant deviations from the power law already set in for about $s = 40$. Thus, data¹¹ for short chains with $N_b < 400$ clearly cannot be taken as a strong evidence for eq 5, because this is less than a decade in s that can be expected to be described by the correct power law. On the other hand, the present numerical data for $400 \leq N_b \leq 6400$ already provide a rather convincing evidence (for $N_b = 6400$, there are two decades in s compatible with the power law). Similar observations have been reported by Wittmer et al.¹⁰ for the case of melts, using chain lengths up to $N_b = 8192$ in this case.

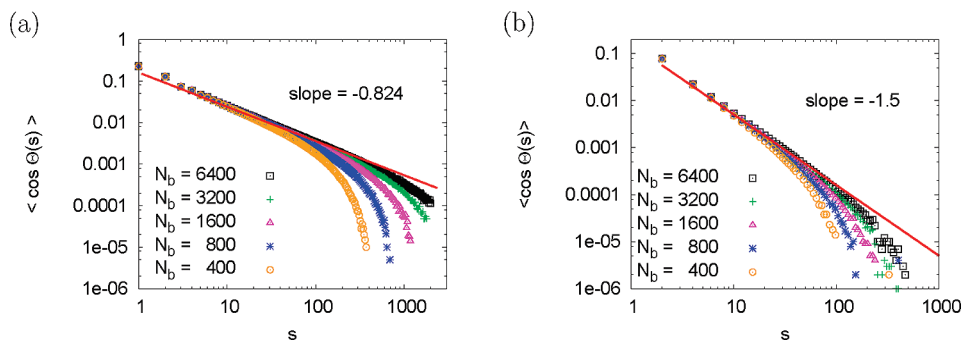


Figure 2. Log–log plot of the bond vector correlation function $\langle \cos \Theta(s) \rangle$ versus the “chemical distance” s along the chain, for the standard SAW model on the simple cubic lattice (a) and for the same model with a nearest-neighbor attraction $\epsilon = k_B T \ln q_\theta$ chosen such that the chain is at the Θ -temperature. Chain lengths from $N_b = 400$ to $N_b = 6400$ are included, as indicated. The straight lines included show simple power laws $\langle \cos \Theta(s) \rangle = 0.16s^{-0.824}$ (a) and $\langle \cos \Theta(s) \rangle = 0.16s^{-1.5}$ (b).

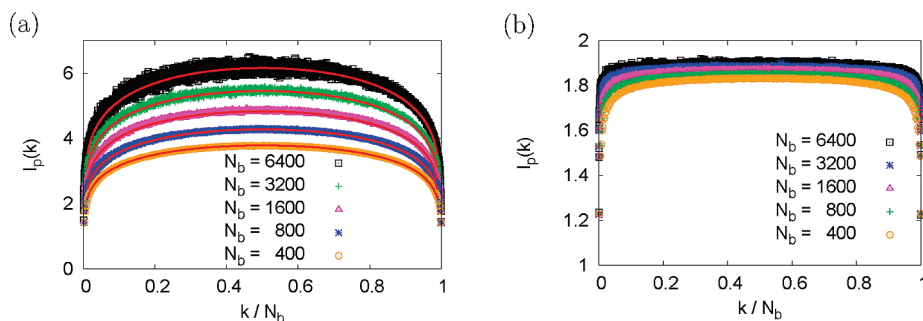


Figure 3. Flory's definition $l_p(k)$ for the local persistence length of a polymer chain (eq 6), plotted as a function of k/N_b for $N_b = 400$ to $N_b = 6400$, as indicated in part a. Part a refers to the standard SAW model on the simple cubic lattice, and solid curves are best fits to eq 7, using $\alpha = 1.6888$ and $\nu = 0.5876$. Part b shows corresponding data for the same model at the Θ temperature (cf. Figure 2b).

Of course, for nonideal chains the product of two bond vectors \vec{a}_i, \vec{a}_k does not only depend on $s = k - i$ but on k as well, and so the precise meaning of $\langle \cos \Theta(s) \rangle$ in Figure 2 is an average along the chain,

$$\langle \cos \Theta(s) \rangle = \sum_{i=1}^{N_b} \langle \cos \Theta_{ik} \rangle / (N_b - s), \quad \langle \cos \Theta_{ik} \rangle = \langle \vec{a}_i \cdot \vec{a}_k \rangle / l_b^2 \quad (22)$$

with $s = |k - i|$. If one would ignore the knowledge that eq 22 is described by the power laws eqs 5, 10 and rather would try to apply eq 1, a failure of eq 1 readily is apparent when one would plot (not shown) $\log \langle \cos \Theta(s) \rangle$ linearly vs s . Rather than observing a straight line (the slope of which would yield l_p/l_b), one finds a rapidly decreasing strongly curved function. Only in the range $N_b/10 < s < N_b/2$ (which corresponds to the range in Figure 2 where the data fall below the power law) could one fit straight lines, but the resulting estimates for l_p would be unreasonably large (and of the order of N_b itself, which shows that such an analysis clearly is invalid). This fact that one cannot extract any meaningful estimate for the persistence length of the SAW model is to be expected, of course, since orientational correlations arise as a consequence of the excluded volume interactions only, for the simple random walk model we would have $\langle \vec{a}_i \cdot \vec{a}_j \rangle = l_b^2 \delta_{ij}$ and hence $l_p = 0$. However, the situation is different for semiflexible polymers, such as bottle-brush polymers (section 3) where an analysis in terms of eq 1 seems to work but nevertheless gives misleading results (depending on N_b and diverging as $N_b \rightarrow \infty$, cf eq 12).

In order to further test eq 7, Figure 3 gives a plot of $l_p(k)$ vs k ; for the good solvent case we fully confirm the conclusions of Schäfer and Elsner,¹⁴ showing with more extensive and precise data than in¹⁴ that eq 7 indeed is a rather accurate approximation.

Thus, while in the Θ solvent case (Figure 3b) the persistence length as defined from eq 6 is constant in the interior part of the chain, and independent of N_b for large N_b , this is not the case for good solvent conditions, where the maximum value (for $k = N_b/2$) diverges for $N_b \rightarrow \infty$, as proposed in eq 9. Since

$$l_p(k)/l_b = \sum_{i=1}^{N_b} \langle \cos \Theta_{ki} \rangle \quad (23)$$

one also finds for the average \bar{l}_p of $l_p(k)$ that

$$\bar{l}_p = \frac{1}{N_b} \sum_{k=1}^{N_b} l_p(k) = l_b \sum_{k=1}^{N_b} \sum_{i=1}^{N_b} \langle \cos \Theta_{ki} \rangle / N_b \quad (24)$$

which reduces to l_p' (eq 11) for $N_b \rightarrow \infty$. Thus, there is no need to separately discuss l_p' here - both l_p' and \bar{l}_p diverge according to eq 12 in the good solvent case as $N_b \rightarrow \infty$.

Finally, we mention that we have not followed up on persistence length definitions based on the structure factor for the SAW: plotting $qS(q)$ vs q one does not find a “Holtzer plateau”, a regime of q with $l_p^{-1} \ll q \ll l_b^{-1}$ does not exist at all here, due to the high flexibility of the SAW.

3. Persistence Lengths for Bottle-Brush Polymers

Using the bond-fluctuation model on the simple cubic lattice, bottle-brush polymers with backbone chain lengths N_b up to $N_b = 1027$ (for side chain length $N \leq 24$) were studied for two grafting densities ($\sigma = 1/2$ and $\sigma = 1$), as well as bottle-brush polymers with $N_b \leq 259$ only but N up to $N = 48$ and $\sigma = 1$. The bond fluctuation model^{46–48} is more complicated than the simple SAW model: each effective monomer blocks all eight corners of an elementary cube of the lattice from further occupation; bond

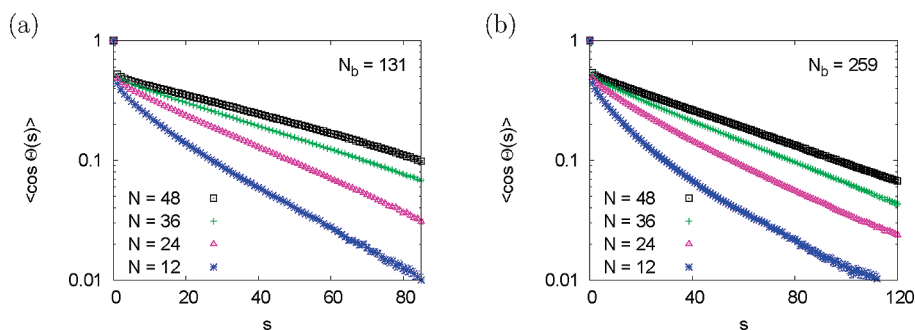


Figure 4. Bond vector correlation function $\langle \cos \Theta(s) \rangle$ of the backbone of the flexible bottle-brush polymers plotted against the “chemical distance” s along the backbone for $N_b = 131$ (a) and $N_b = 259$ (b). Various values of side chain length N are shown, as indicated. Note the semilog scales of the plot, implying that a law $\exp(-s/\ell_p)$ could be a simple straight line.

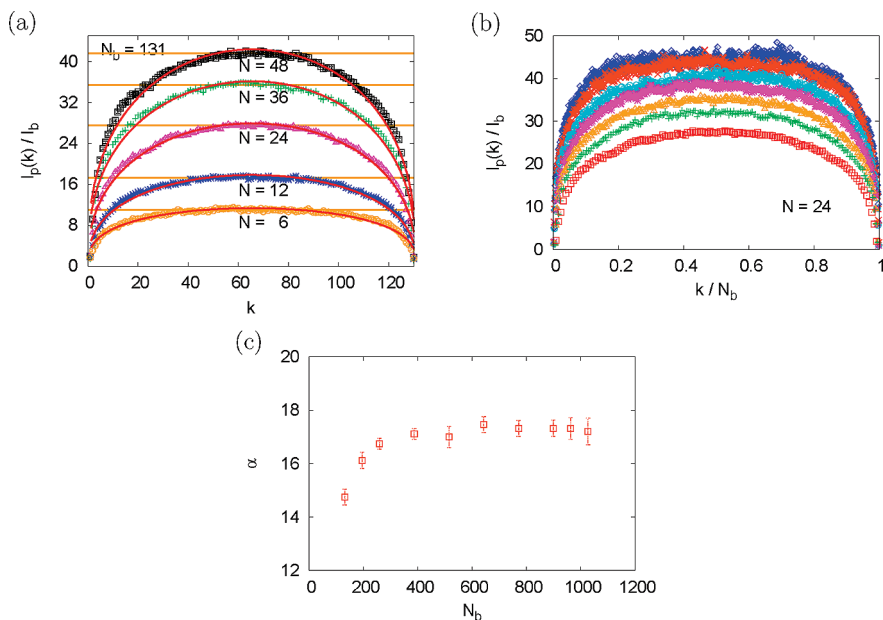


Figure 5. Local persistence length $\ell_p(k)$ plotted vs k for $N_b = 131$ (a) side chain lengths $N = 6, 12, 24, 36,$ and 48 are shown (from bottom to top). In part a, dotted horizontal curves (plateau) indicate estimates $\ell_p^{(1)}$ of the persistence length (Table 1) and solid curves are fits to $\ell_p(k)/\ell_b = \alpha[k(N_b - k)/N_b]^{2\nu-1}$, cf. eq 7. The values of the parameters α and ν are listed in Table 2. Part b shows $\ell_p(k)$ plotted vs k/N_b for fixed side chain length $N = 24$ and several choices of the backbone length, namely $N_b = 131, 195, 259, 387, 515, 771,$ and 1027 from bottom to top. Part c shows a plot of α vs N_b when the simulation data are fitted to eq 7 in the range $0.3 < k/N_b < 0.7$.

vectors \vec{a} are taken from the set $(\pm 2, 0, 0), (\pm 2, \pm 1, 0), (\pm 2, \pm 1, \pm 1), (\pm 2, \pm 2, \pm 1), (\pm 3, 0, 0), (\pm 3, \pm 1, 0)$, and all permutations thereof (the lattice spacing still is the unit of length). The reason for using this model is the existence of a very efficient simulation algorithm,⁴⁹ by combining the “L26 move”¹⁰ and “pivot moves”⁴⁴ dynamic Monte Carlo sampling is able to generate statistically independent configurations of the bottle-brush polymer relatively fast. The “L26”-move means that an effective monomer is randomly chosen and considered for a jump by a randomly chosen distance vector from the set $(\pm 1, 1, 0, 0)$ or $(\pm 1, \pm 1, 0)$ [or permutations thereof] or $(\pm 1, \pm 1, \pm 1)$. The move is carried out only if both excluded volume and bond length constraints are respected. The key point of this move is that it allows for crossings of bonds during the move; no such simple moves that allow bond crossing for the simple SAW model of the previous sections are known. Without the possibility of bond crossing, two side chains of the bottle-brush that happen to be entangled with each other would relax this topological constraint only extremely slowly.

Two types of “pivot moves” are used: either a randomly chosen monomer of a randomly chosen side chain is used to act as a pivot point, from which the remainder of the side chain (from the pivot point to the free end) is rotated by a randomly chosen orientation

allowed by the lattice symmetry; or a randomly chosen monomer of the backbone is used to carry out such a random orientation change of the (smaller) part of the whole bottle-brush (see ref 49 for implementation details).

As an example of typical results, Figure 4 shows a plot of $\langle \cos \Theta(s) \rangle$ of the backbone versus the “chemical distance” s (note that $\ell_b \approx 2.7$ lattice spacings for the bond fluctuation model⁴⁸), in order to test for the applicability of eq 1. While for short side chain lengths ($N = 12$) there is pronounced curvature on the semilog plot, similar as in the case of the simple linear chain (SAW model), for longer side chains (particularly for $N_b = 259$) a fit to an exponential decay, for large s (but not too large $s, s < N_b/2$) is feasible. But the resulting persistence lengths ℓ_p do depend strongly on the backbone length (see Table 1). The same conclusion results when eq 6 is used (Figure 5). Although the estimates ℓ_p extracted from the plateau in Figure 5 and from the fit to an effective exponential decay are always compatible with each other, they are not meaningful estimates of the local intrinsic stiffness of the chains, since they depend strongly on N_b . Qualitatively, the behavior of $\ell_p(k)$ is always very similar to the simple SAW model, although now the persistence lengths are much larger, cf. Figure 3. When one compares the numbers for the exponent ν resulting from the simple fitting procedure (Table 2),

one notes however that ν for $N_b \leq 259$ is systematically too large, indicating that all data are still in a preasymptotic regime, much longer N_b is necessary to see the asymptotic scaling behavior. Figure 5b tests the variation of $\ell_p(k)$ with N_b for fixed side chain length, $N = 24$. Fitting these data to the theoretical expressions eq 7 and imposing $\nu = 0.588$ we obtain the dependence of the prefactor α on N_b . The asymptotic region where α is independent of N_b is only reached for $N_b > 400$. (Figure 5c). Figure 6 now shows a test of eq 14, including much larger values of N_b (but smaller N) to ensure that the asymptotic scaling regime is reached. Indeed it is found that the larger N the larger N_b must be to see that the data settle down to straight line behavior, as is implied when eq 14 is valid. The resulting estimates for ℓ_p'' are by construction independent of N_b , and hence more serious candidates for a measure of local intrinsic stiffness of the bottle-brush than the estimates ℓ_p and $\ell_{p,\max}(k)$ derived from Figures 4 and 5, of course. It is gratifying to note from Figures 5c and 6a that both eqs 7 and 14 reach their asymptotic regime of validity in the same range of values for N_b , namely $N_b \geq 400$ for $N = 24$. From the estimates of the persistence length ℓ_p'' listed in Table 3 we can conclude that bottle brushes under good solvent conditions behave like standard self-avoiding walks if their contour length N_b/b is of the order of 100 persistence lengths.

Figures 7–9 test the idea to estimate persistence lengths from the onset of the “Holtzer plateau”. One recognizes immediately that the total scattering $qS(q)$ from bottle-brush polymers under

Table 1. Persistence Lengths $\ell_p^{(1)}$ Determined by the Values of Plateau in Figure 5, and ℓ_p'' Calculated by Using Equation 11 (See Figure 4) for Bottle-Brush Polymer of Backbone Length N_b and Side Chain Length N , Where $b_b = 2.7$

N_b		$N = 6$	$N = 12$	$N = 24$	$N = 36$	$N = 48$
259	$\ell_p^{(1)}/b_b$	13.01	20.43	34.52	47.01	57.01
	ℓ_p''/b_b	14.45	20.42	33.80	44.02	54.00
195	$\ell_p^{(1)}/b_b$	12.20	19.25	31.92	42.88	52.8
	ℓ_p''/b_b	13.19	19.43	31.63	42.88	52.13
131	$\ell_p^{(1)}/b_b$	10.98	17.28	27.52	35.42	41.58
	ℓ_p''/b_b	11.80	17.88	28.20	37.76	44.55
99	$\ell_p^{(1)}/b_b$	10.30	15.55	24.15	31.40	38.20
	ℓ_p''/b_b	10.88	16.50	25.71	33.20	38.20
67	$\ell_p^{(1)}/b_b$	8.93	13.15	18.78	24.50	28.72
	ℓ_p''/b_b	9.78	14.41	21.04	28.72	28.72

Table 2. Fitting Parameters α and ν of Equation 7 for Bottle-Brush Polymer of Backbone Lengths $N_b = 131$ and $N_b = 259$ and Side Chain Lengths $N = 6, 12, 24, 36$ and 48

N_b		$N = 6$	$N = 12$	$N = 24$	$N = 36$	$N = 48$
131	α	3.340	4.474	6.672	9.198	11.090
	ν	0.675	0.698	0.705	0.696	0.692
259	α	4.252	5.539	8.641	10.502	13.325
	ν	0.637	0.660	0.672	0.682	0.676

good solvent conditions never exhibits a “Holtzer plateau”, irrespective of N_b and N . Also when the side chain length is too short ($N = 6, 12$), the structure factors $qS_b(q)$, $qS(q)/S_{cs}(q)$, and $qS(q)/S_{cs}^m(q)$ never become really horizontal over an extended regime. Here $S_b(q)$ is the structure factor due to the monomers contained in the actual backbone of the bottle-brush polymer, so this structure factor is precisely defined without any ambiguity. It shows rather well-defined horizontal regions, i.e. the “Holtzer plateau”, when the side chain length is large enough, $N = 24$ or $N = 48$. This indicates that the expected stiffening of the backbone due to the grafted side chains indeed is visible for these side chain lengths.

While $S_b(q)$ is straightforward to obtain in a simulation, it is very difficult to obtain from experiment (one needs to carry out small angle neutron scattering using polymers with deuterated backbones but protonated side chains, to single out the coherent scattering contribution from the backbone only). So in most experiments one tries to estimate the backbone scattering indirectly, by “dividing out” the scattering from the side chains from the total structure factor. The side chain scattering is approximately described by the “cross-sectional structure factor” $S_{cs}(q)$, which is related to the radial density profile $\rho(r)$ in the plane perpendicular to the (local) backbone direction. Now the problem to define the perpendicular direction for a undulating linear object such as the backbone of a bottle-brush polymer is somewhat subtle,¹⁵ but if the backbone chains are sufficiently stiff due to the side chains, one can obtain $\rho(r)$ with reasonable accuracy. It was found that $\rho(r)$ for bottle-brush polymers with flexible backbones is very similar to the density profile $\rho_{\text{stiff}}(r)$ for bottle-brushes with strictly rigid backbones, and well described by a function $h(r)$ ^{16,50}

$$\rho(r) \approx h(r) = \frac{c}{1 + (r/r_1)^{x_1}} \exp[-(r/r_2)^{x_2}] \quad (25)$$

with c a normalization constant, $x_1 = (3\nu - 1)/2\nu$, $x_1 \approx 3$, and r_1, r_2 two characteristic lengths (see ref.^{16,50} for details). The cross-sectional scattering then is defined by^{24–27}

$$S_{cs}(q) = \frac{|\int_0^\infty r dr \rho(r) J_0(qr)|^2}{|\int_0^\infty dr r \rho(r)|^2} \quad (26)$$

where $J_0(r)$ is the zeroth order Bessel function of the first kind. Using the $\rho(r)$ as actually observed in the simulation to compute

Table 3. Persistence Lengths ℓ_p'' (σ, N) Determined by Equation 14 and 15 for the Grafting Densities $\sigma = 1$ and $1/2$ and the Side Chain Lengths $N = 0, 6, 12, 18$, and 24 (see Figure 6)

	$N = 0$	$N = 6$	$N = 12$	$N = 18$	$N = 24$
ℓ_p'' ($\sigma = 1, N$)	1.15	6.43	10.30	14.15	17.55
ℓ_p'' ($\sigma = 1.2, N$)	1.15	4.34	6.65	8.54	10.48

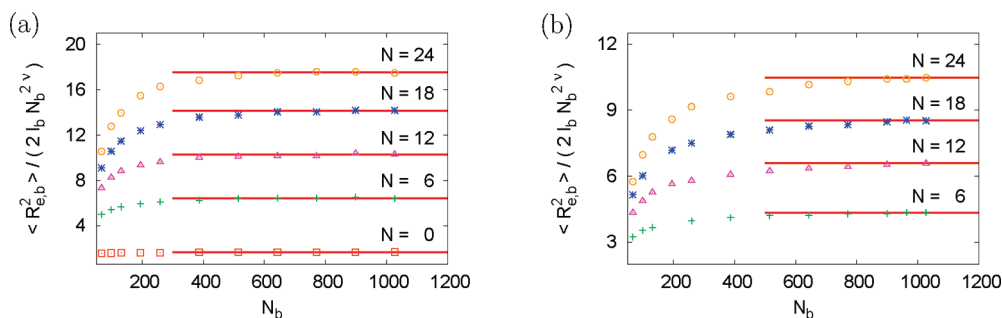


Figure 6. Rescaled mean square end-to-end distance $\langle R_{e,b}^2 \rangle / (2 l_b N_b^{2\nu})$ plotted against backbone length N_b for bottle-brush polymers with grafting density $\sigma = 1$ (a) and $\sigma = 1/2$ (b). Various values of side chain length N are shown ($N = 0$ means that no side chains are grafted at all). Horizontal straight lines indicate estimates for ℓ_p'' (Table 3).

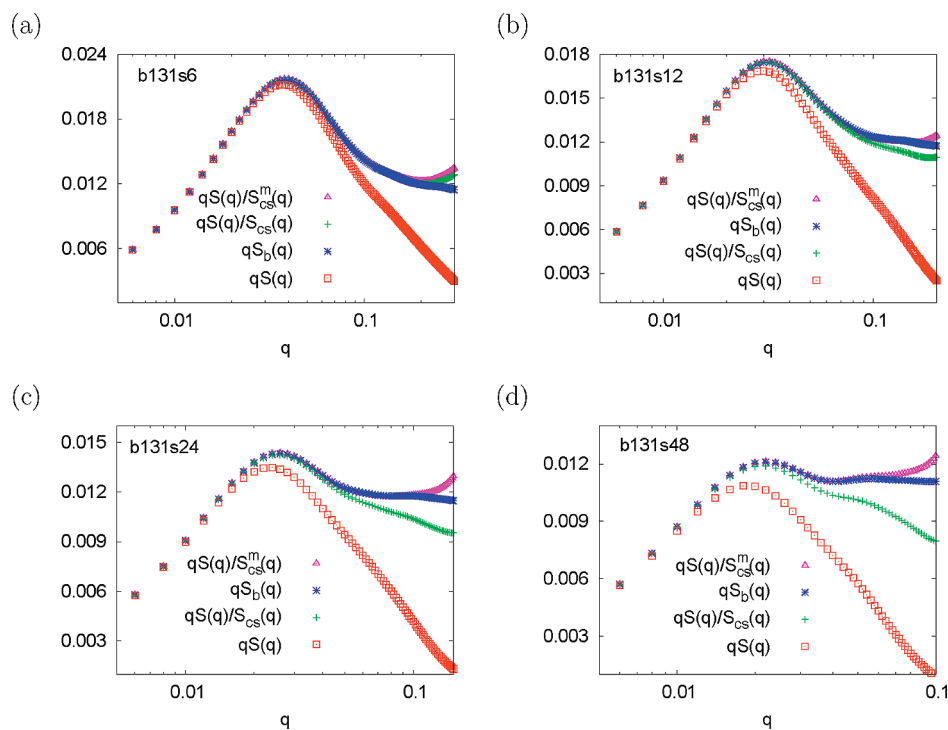


Figure 7. Rescaled normalized structure factors $qS(q)$ of the total bottle-brush, $qS_b(q)$ of the backbone, $qS(q)/S_{cs}(q)$ where $S_{cs}(q)$ is the cross-sectional structure factor, and $qS(q)/S_{cs}^m(q)$ where $S_{cs}^m(q)$ is the modified cross-sectional structure factor (see text). All data are for $N_b = 131$ and side chain lengths $N = 6$ (a), $N = 12$ (b), $N = 24$ (c), and $N = 48$ (d).

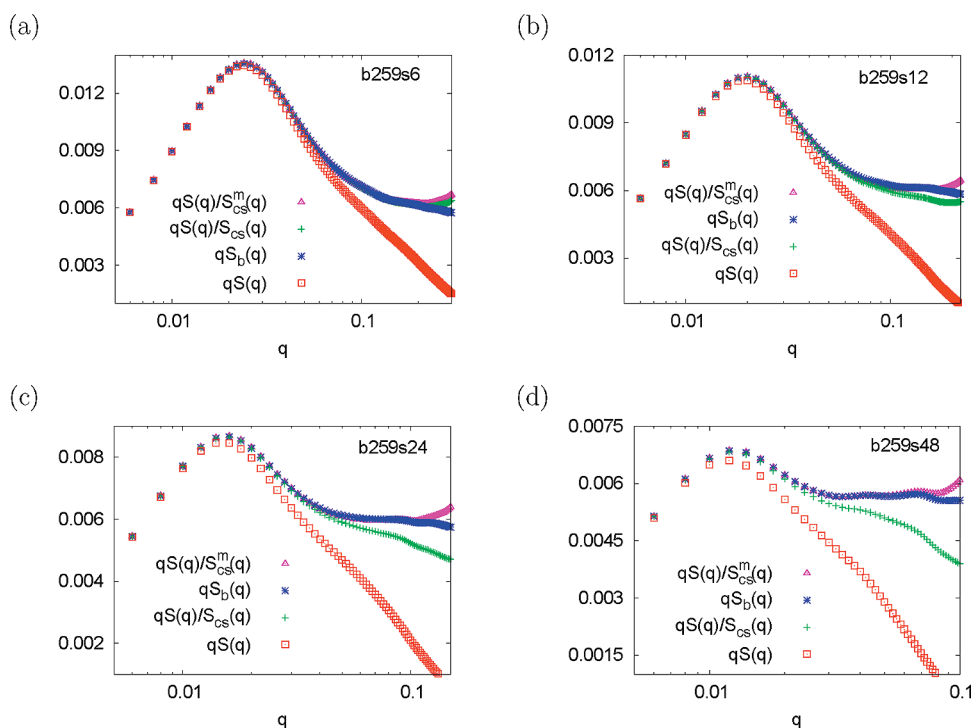


Figure 8. Same as Figure 7, but for $N_b = 259$. Note that the plateau values (π/L_{bb}) in Figures 7 and 8 determine the contour length L_{bb} of the backbone and the position q^* where the plateau starts to develop yields another estimate of the persistence length l_p^* ($q^* = 3.5/l_p^*$).

$S_{cs}(q)$ no “Holtzer plateau” is observed, however. Only when we “redefine” the side-chain scattering via

$$S_{ss}(q) \equiv S(q)/S_b(q) \quad (27)$$

and choose a function $h(r)$ that fits {identifying $S_{cs}(q) = S_{ss}(q)$ } $S_{ss}(q)$ near the region where $qS(q)/S_b(q)$ has its maximum are we

able to obtain a well-defined plateau again. This way of defining an effective cross-sectional scattering is included in Figures 7, 8 (denoted as $S_{cs}^m(q)$).

Table 4 collects the resulting estimates for L_{bb} and l_p^* (note that for $N = 6$ and $N = 12$ we have defined L_{bb} from the minimum of $qS_b(q)$ vs q). One sees that L_{bb} is roughly independent of N , which is reasonable, and that $L_{bb} < N_b/b$, which is also reasonable, since

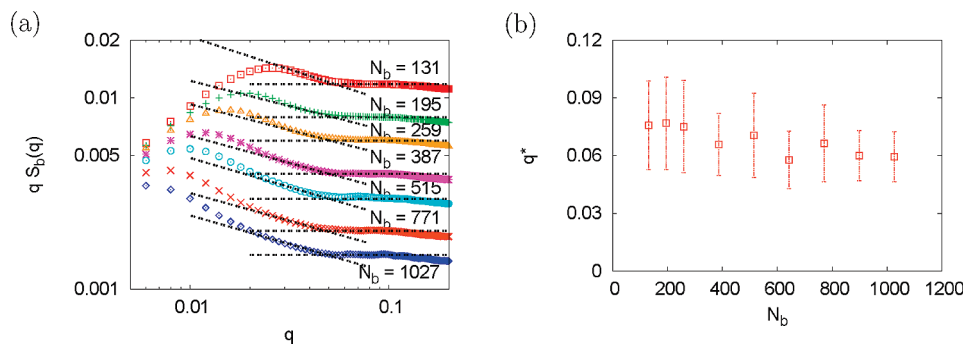


Figure 9. (a) Log–log plot of $qS_b(q)$ vs q for $N = 24$ and backbone chain lengths $N_b = 131, \dots, 1027$, as indicated. Broken straight lines indicate fits to estimate the onset value q^* of the “Holtzer plateau”. (b) Plot of q^* vs N_b .

Table 4. Contour Lengths L_{bb} and Persistence Lengths $l_p^* = 1/q^*$ Determined by the Scattering Functions of Backbone $S_b(q)$ for Bottle-Brush Polymers of Backbone Lengths $N_b = 131$ and $N_b = 259$ and Side Chain Lengths $N = 6, 12, 24, 36$, and 48 , Using the Same Method As Shown in Figure 9a

N_b		$N = 6$	$N = 12$	$N = 24$	$N = 48$
131	L_{bb}	266.24	258.56	267.37	281.76
	l_p^*	7.18	11.07	18.59	27.58
259	L_{bb}	508.35	510.50	526.67	556.03
	l_p^*	9.01	13.05	19.57	35.91

there are local fluctuations of the actual backbone with respect to the coarse-grained backbone (Figure 1). Gratifyingly, there is not much of a dependence of L_{bb} on side chain length. But also this method yields estimates l_p^* strongly dependent on the backbone length, as expected, since from Figures 5c and 6 we know that much larger values of N_b are needed to reach the asymptotic regime. Thus, Figure 9 focuses on the Holtzer plots for $N = 24$ but a wide range of N_b (considering the backbone structure factor $S_b(q)$ only). In order to define a value q that unambiguously marks the onset of the Holtzer plateau, we tried different methods to extract the crossover point. The first method consists of fitting two straight lines to $qS_b(q)$ (in a log–log plot) near the onset of the Holtzer plateau and determining q^* from the intersection point (this is shown in Figure 9a). The second method consists of fitting algebraic crossovers of the form $a + bq^{-1} + cq^{-2} + dq^{-3}$ or simply $a + bq^{-1} + cq^{-2}$ to the crossover regime. These functions show a shallow minimum, and we identify the position of this minimum as $1/q^*$. All methods yield different results, albeit with the same trend: a slight decrease of q^* at small N_b and a saturation at large N_b . In Figure 9b we show the average q^* value we obtained and give error bars encompassing the variation between the different methods to determine this value. The figure shows that q^* is independent of N_b for $N_b > 600$, and hence it does measure an intrinsic property of bottle-brush polymers, for long enough backbones. If one follows Lecommandoux et al.¹⁹ to estimate the persistence length l_p^* from q^* via $l_p^* = 3.5/q^*$, one would get $l_p^* \approx 60$ from Figure 9b. On the other hand, using $\langle R_{e,b}^2 \rangle / (l_p N_b^{2\nu}) = 2/l_p$ [cf. eqs 14 and 15] one would extract $l_p \approx 18$ from Figure 6a; thus, it may be better to simply take $l_p^* = 1/q^*$, in order to obtain mutually consistent definitions of an “intrinsic” persistence length.

4. Conclusions

In the present work, computer simulations of models for flexible and semiflexible macromolecules were presented, and the question was considered to what extent different definitions of the persistence length yield information on the local “intrinsic” stiffness of the polymer chains or reflect global conformational properties. As an extreme case of a fully flexible macromolecule, the self-avoiding walk on the simple cubic lattice was studied,

both in the athermal case (which means very good solvent conditions) and under Θ conditions. As a model for semiflexible polymers, bottle-brush polymers were considered; there the chain stiffness of the backbone can be changed to a large extent by varying the length of the side chains. The choice of this particular polymer architecture was motivated by the fact that in the experimental literature a controversial discussion about the persistence lengths of bottle-brushes can be found. Only the experimentally relevant case of good solvent conditions was studied in this case.

Using the PERM algorithm, we have been able to obtain very accurate results for the self-avoiding walk model on the simple cubic lattice, for chain lengths up to $N = 6400$, both for the athermal model, and at the Θ point. For the self-avoiding walk (SAW) model under good solvent conditions, it was verified that orientational correlations between bond vectors show a power law decay, $\langle \cos \Theta(s) \rangle \propto s^{-\beta}$ with $\beta = 2 - 2\nu$, for $1 \ll s \ll N_b$, while at the Θ point the decay law is faster, $s^{-3/2}$ {eqs 5 and 10}. Since deviations from the power law due to finite chain lengths occur already for $s \approx N_b/10$, availability of numerically accurate results for very long chains, as presented here, has been crucial for these conclusions. In both cases, the assumption of an exponential decay {eq 1} is unsuitable: it can describe at best the decay at rather large s , and the decay length is not related to the range of the intrinsic stiffness of the chain (which is very small for this model). The definition of the persistence length in terms of a projection of bond vectors \vec{a}_k on the end-to-end distance, in the good solvent case is found to be well described by the prediction due to Schäfer et al.,¹⁴ eq 7. This result implies a divergence of the persistence length as $N \rightarrow \infty$, eq 9, and hence is not at all related to the local intrinsic stiffness of the chain. We show that this result can be carried over to bottle-brush polymers: eq 7 provides a very good fit of $l_p(k)$ as well; due to the local stiffness of bottle-brush polymers, caused by dense grafting of side chains, the prefactor α in eq 7 is much larger than for the simple SAW, and increases with increasing side chain length N . We demonstrate (Figure 6) that bottle-brush polymers for large enough backbone lengths N_b show standard scaling like SAW’s, eq 14, but with a strongly enhanced prefactor, which can be used as a reasonable measure to define a range of intrinsic stiffness (l_p^*) that does not depend on N_b , and would reduce to the ordinary definition of the persistence length for Gaussian chains.

We show that in typical cases the SAW scaling limit is reached if the contour length N_b/l_b of the bottle brush exceeds this intrinsic persistence length l_p^* by about a factor of 100. Note that although with increasing side chain length N this intrinsic persistence length l_p^* increases strongly (Table 3), the excluded volume interaction does not become irrelevant, since the cross-sectional radius R_{cs} (Figure 1) also increases. We show also that a persistence length extracted from the apparent exponential decay of the orientational correlation function at intermediate values of s (Figure 4) depends strongly on N_b and is not a characteristic of

the internal stiffness of the bottlebrush, unlike ρ_p'' . Of course, in the context of analytical calculations one can define an “intrinsic” persistence length l_p in terms of a bending modulus $\kappa = k_B T l_p$, that appears as a prefactor of a term in a suitable effective Hamiltonian,^{30,51} but then the problem arises to relate κ to quantities immediately observable in simulation or experiment. As an alternative way to estimate the range of intrinsic stiffness, we discuss the onset of the “Holtzer plateau” in the normalized scattering due to the backbone of the bottle-brushes, $qS_b(q)$ {Figures 7–9}. We show that the wavenumber q^* characterizing this onset for large enough N_b becomes independent of N_b , and hence one can conclude that $l_p^* \propto 1/q^*$ also is a useful measure for the range of the intrinsic chain stiffness. We expect that these considerations will help the interpretation of corresponding experiments, where so far the problem that (depending on the method of data analysis and the conditions of the experiment) the persistence length is not an intrinsic property of the respective polymer often has not been recognized.

Acknowledgment. This work has been supposed by the Deutsche Forschungsgemeinschaft (DFG) under grant No SFB 625/A3 and by the European Science Foundation (ESF) under the STIPOMAT program. We are grateful to H. Meyer, S. Rathgeber, and M. Schmidt, and J. P. Wittmer for stimulating discussions. The computer simulations were carried out on the Juropa supercomputer and the SoftComp NoE computer cluster at the Jülich Supercomputing Centre. We thank the John von Neumann Institute for Computing for the allocation of computing time.

References and Notes

- Grosberg, A. Yu.; Khokhlov, A. R. *Statistical Physics of Macromolecules*; AIP Press: New York, 1994.
- Rubinstein, M.; Colby, R. H. *Polymer Physics*; Oxford Univ. Press: Oxford, U.K., 2003.
- Des Cloizeaux, J.; Jannink, G. *Polymers in Solution: Their Modeling and Structure*; Clarendon Press: Oxford, U.K., 1990.
- Kratky, O.; Porod, G. *Recl. Trav. Chim.* **1949**, *68*, 1106.
- Duplantier, B. *J. Chem. Phys.* **1987**, *86*, 4233.
- Schäfer, L., *Excluded Volume Effects in Polymer Solutions as Explained by the Renormalization Group*; Springer: Berlin, 1999.
- Flory, P. J. *Principles of Polymer Chemistry*; Cornell Univ. Press: Ithaca, NY, 1953.
- DeGennes, P. G. *Scaling Concepts in Polymer Physics*; Cornell University Press: Ithaca, NY, 1979.
- Wittmer, J. P.; Meyer, H.; Baschnagel, J.; Johner, A.; Obukhov, S.; Mattioni, L.; Müller, M.; Semenov, A. N. *Phys. Rev. Lett.* **2004**, *93*, 147801.
- Wittmer, J. P.; Becknich, P.; Meyer, H.; Cavallo, A.; Johner, A.; Baschnagel, J. *Phys. Rev. E* **2007**, *76*, 011803.
- Shirvanyants, D.; Panyukov, S.; Liao, Q.; Rubinstein, M. *Macromolecules* **2008**, *41*, 1475.
- Flory, P. J. *Statistical Mechanics of Chain Molecules*; Interscience: New York, 1969.
- Yamakawa, H. *Modern Theory of Polymer Solutions*; Harper and Row: New York, 1971.
- Schäfer, L.; Elsner, K. *Eur. Phys. J E* **2004**, *13*, 225. Schäfer, L.; Ostendorf, A.; Hager, J. *J. Phys. A: Math. Gen.* **1999**, *32*, 7875.
- Hsu, H.-P.; Binder, K.; Paul, W. *Phys. Rev. Lett.* **2009**, *103*, 198301.
- Hsu, H.-P.; Paul, W.; Rathgeber, S.; Binder, K. *Macromolecules* **2010**, *43*, 1592.
- In ref 16, the factor $1/3$ in eq 15 was absorbed in the definition of ρ_p'' .
- Des Cloizeaux, J. *Macromolecules* **1973**, *6*, 403.
- Lecommandoux, S.; Chiécot, F.; Barsali, R.; Schappacher, M.; Deffieux, A.; Brület, A.; Cotton, J. P. *Macromolecules* **2002**, *35*, 8878.
- Zhang, M.; Müller, A. H. E. *J. Polym. Sci., Part A: Polym. Chem.* **2005**, *43*, 3461.
- Sheiko, S. S.; Sumerlin, B. S.; Matyjaszewski, K. *Prog. Polym. Sci.* **2008**, *33*, 759.
- Neugebauer, T. *Ann. Phys. (Leipzig)* **1943**, *434*, 509.
- Holtzer, A. *J. Polym. Sci.* **1955**, *17*, 432.
- Zhang, B.; Gröhn, F.; Pedersen, J. S.; Fischer, K.; Schmidt, M. *Macromolecules* **2006**, *39*, 8440.
- Pedersen, J. S.; Schurtenberger, P. *Macromolecules* **1996**, *29*, 7602.
- Rathgeber, S.; Pakula, T.; Matyjaszewski, K.; Beers, K. L. *J. Chem. Phys.* **2005**, *122*, 124904.
- Fenz, L.; Strunz, P.; Geue, T.; Textor, M.; Borsiov, O. *Eur. Phys. J. E* **2007**, *23*, 237.
- Birshstein, T. M.; Borisov, O. V.; Zhulina, E. B.; Yurasova, T. A. *Polym. Sci. USSR* **1987**, *29*, 1293.
- Lipson, J. E. G. *Macromolecules* **1993**, *26*, 203.
- Fredrickson, G. H. *Macromolecules* **1993**, *26*, 2825.
- Zhulina, E. B.; Vilgis, T. A. *Macromolecules* **1995**, *28*, 1008.
- Rouault, Y.; Borisov, O. V. *Macromolecules* **1996**, *29*, 2605.
- Saariaho, M.; Ikkala, O.; Szleifer, I.; Erukhimovich, I.; ten Brinke, G. *J. Chem. Phys.* **1997**, *107*, 3267.
- Shiokawa, K.; Itoh, K.; Nemoto, M. *J. Chem. Phys.* **1999**, *111*, 8165.
- Subbotin, A.; Saariaho, M.; Ikkala, O.; ten Brinke, G. *Macromolecules* **2000**, *33*, 3447.
- Nakamura, Y.; Norisuye, T. *Polym. J.* **2001**, *33*, 874.
- Elli, S.; Ganazzoli, F.; Timoshenko, E. G.; Kuznetsov, Y. A.; Connolly, R. *J. Chem. Phys.* **2004**, *120*, 6257.
- Connolly, R.; Bellesia, G.; Timoshenko, E. G.; Kuznetsov, Y. A.; Elli, S.; Ganazzoli, F. *Macromolecules* **2005**, *38*, 5288.
- Yethiraj, A. *J. Chem. Phys.* **2006**, *125*, 204901.
- Allison, S. A.; Sorlie, S. S.; Pecora, R. *Macromolecules* **1990**, *23*, 1110.
- Hakansson, C.; Elvingson, C. *Macromolecules* **1994**, *27*, 3843.
- Gunari, N.; Schmidt, M.; Janshoff, A. *Macromolecules* **2006**, *39*, 2219.
- Bolisetty, S.; Airaud, C.; Xu, Y.; Müller, A. H. E.; Harnau, L.; Rosenfeldt, S.; Lindner, P.; Ballauff, M. *Phys. Rev. E* **2007**, *75*, 040803(R).
- Sokal, A. D. In *Monte Carlo and Molecular Dynamics Simulations in Polymer Science*, Binder, K., Ed.; Oxford Univ. Press: New York, 1995; p 47.
- Grassberger, P. *Phys. Rev. E* **1997**, *56*, 3682.
- Carmesin, I.; Kremer, K. *Macromolecules* **1988**, *21*, 2819.
- Deutsch, H. P.; Binder, K. *J. Chem. Phys.* **1991**, *94*, 2294.
- Paul, W.; Binder, K.; Heermann, D. W.; Kremer, K. *J. Phys. II (Fr.)* **1991**, *1*, 37.
- Hsu, H.-P.; Paul, W.; Binder, K. To be published.
- Hsu, H.-P.; Paul, W.; Binder, K. *J. Chem. Phys.* **2008**, *129*, 204904.
- Kroy, K.; Frey, E. *Phys. Rev. Lett.* **1996**, *77*, 306.